Available online at www.sciencedirect.com
ScienceDirect
Thin Solid Films 516 (2008) 5654–5658
www.elsevier.com/locate/tsf

Preparation and characteristics of poly(amide–imide)/titania nanocomposite thin films

Mei-Hui Tsai [a,*], Chi-Jung Chang [b], Pei-Jyun Chen [a], Cheng-Jung Ko [a]

[a] Department of Chemical and Materials Engineering National Chin-Yi University of Technology Taichung 41111, Taiwan, ROC
[b] Department of Chemical Engineering Feng Chia University Taichung 40724, Taiwan, ROC

Available online 13 July 2007

Abstract

Poly(amide–imide)/titania (PAI/TiO_2) nanocomposite has been successfully fabricated through the in situ formation of TiO_2 within a PAI matrix by sol-gel process. Poly(amide amic acid) solutions are prepared by mixing 3,3′,4,4′-benzophenone tetracarboxylic dianhydride (BTDA), 2,2-bis[4-(4-aminophenoxy)phenyl]propane (p-BAPP), trimellitic anhydride chloride (TMAC) and *N*,*N*-dimethyl formamide (DMF) solvent. Tetraethyl orthotitanate ($Ti(OEt)_4$) and actylacetone (ACAC), the latter one is used as chelating agent, are then added to the poly(amide amic acid). Through the sol-gel process and imidization reaction, the PAI/TiO_2 nanocomposite films are formed. In this study, the addition of TMAC to the PAI/TiO_2 nanocomposite films is employed to provide the intermolecular hydrogen bonded between the PAI and PAI or titania. The TiO_2 particle sizes of PAI/TiO_2 (TiO_2 is 8.12 wt. %) are between 40 and 90 nm by the transmission electron microscope (TEM) measurement. Based on X-ray photoelectron spectroscopic (XPS) analysis, the TiO_2 content on the surface of PAI/TiO_2 is higher than that of pure polyimide/titania (PI/TiO_2) nanocomposite film. Thermal decomposition temperatures (T_d), at 5 wt.% loss, are above 460 °C of PAI/TiO_2 and PI/TiO_2 nanocomposite films. The dynamic mechanical analysis (DMA) of the PAI/TiO_2 and PI/TiO_2 nanocomposite films with higher TiO_2 content possesses superior mechanical properties and glass transition temperatures.

Keywords: Poly(amide imide); Titania; Sol-gel; Hydrogen bond; Nanocomposite

1. Introduction

In the past two decades, organic/inorganic nanocomposite materials prepared by sol-gel process have drawn a great deal of attention in material science because of their unique properties [1]. Poly(amide–imide) (PAI) contains both amide and heterocycle imide structures along the main chain of the polymer backbone and possesses high thermal stability, good chemical resistance, excellent mechanical properties and hydrogen bonding interaction [2], being a promising matrix candidate for hybrid materials. In inorganic nanoparticles, TiO_2 is one of the most potential materials in research and application fields because of its versatile functions. Due to the expected properties of TiO_2, considerable attention has been devoted to the manufacture of well-dispersed TiO_2 in polymer matrix used as interference filter, antireflective coating, and optical waveguides [3–5].

Generally, these polymer/inorganics hybrid materials can effectively increase the mechanical and thermal properties by the microstructure of inorganics particles well-dispersing in polymer matrices. In this study, when titanium alkoxide is added into PAI and polyimide (PI) matrix, the gelation and phase separation occurred easily due to the relatively fast hydrolysis rate to produce precipitates of titanium alkoxides. Therefore, the use of acetylacetone (ACAC) chelating agent is necessary in order to control the reactivity of titanium alkoxides of the resulting nanocomposite materials [6–8]. PAI/TiO_2 hybrid films via sol-gel process in situ preparation exhibit higher glass transition temperature, an increase and flattening of the rubbery plateau modulus, and a decrease in crystallinity [9] and could be dried afterwards without any post-treatment utilized in gas separation [10]. Until now, many reports are published about polymer based nano-TiO_2 composites, but the works are rare and lack of systematic compares on poly(amide–imide)/TiO_2 and polyimide/TiO_2 nanocomposite films.

The objective here is to inspect the correlation between the PAI/TiO_2 hybrid film properties and the contents of TiO_2. The

* Corresponding author. Tel.: +886 4 23924505; fax: +886 4 23926617.
E-mail address: tsaimh@ncut.edu.tw (M.-H. Tsai).

0040-6090/$ - see front matter © 2007 Elsevier B.V. All rights reserved.
doi:10.1016/j.tsf.2007.07.033

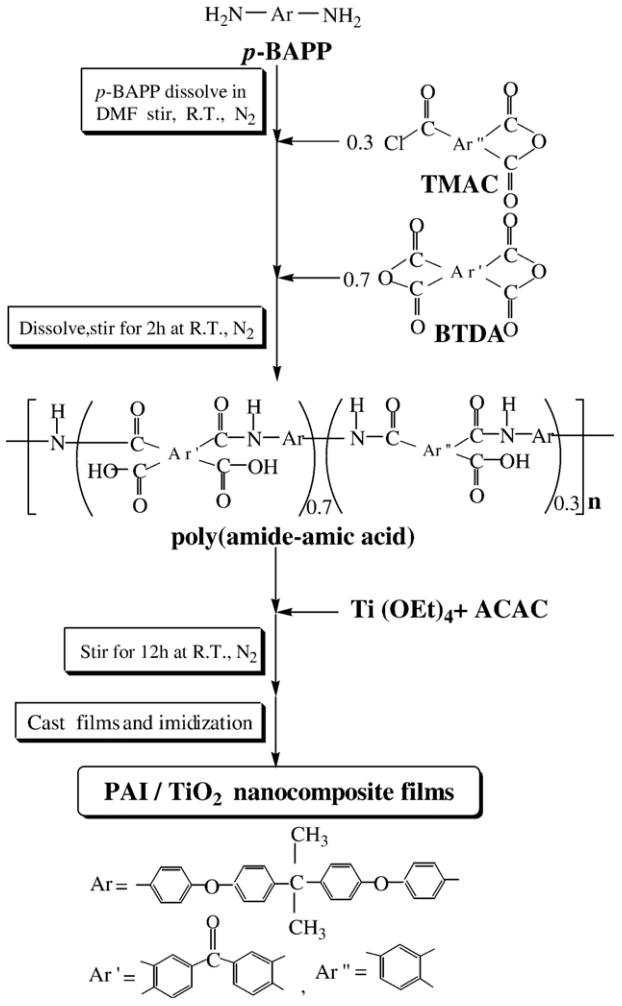

Fig. 1. The flowchart of the procedures to prepare the PAI/TiO_2 nanocomposite films.

effects of TMAC and TiO_2 content of PAI/TiO_2 on the chemical composition of surface, dynamic mechanical properties, thermal degradation, TiO_2 domain size and morphology of nanocomposite films are analyzed by XPS, DMA, TGA, TEM, and SEM, respectively. And further, the above-mentioned characteristics of PAI/TiO_2 and PI/TiO_2 are compared.

2. Experiments

2.1. Materials

2,2-bis[4-(4-Aminophenoxy)phenyl]propane (p-BAPP, 98%) from Aldrich Chemical Company is dried in a vacuum oven at 85 °C for 8 h prior to use. 3,3′, 4,4′-benzophenonetetracarboxylic dianhydride (BTDA) from ACORS Company is purified by recrystallization from acetic anhydride and then dried in a vacuum oven at 120 °C overnight. The titania additive of tetraethyl orthotitanate ($Ti(OEt)_4$), acetylacetone (ACAC) and trimellitic anhydride chloride (TMAC) from Tokyo Chemical Industry (TCI) are used as supplied. *N*,*N*-dimethyl formamide (DMF) from Tedia Company is dehydrated with molecular sieves.

2.2. Synthesis

The flowchart of the procedures to prepare the PAI/TiO_2 nanocomposite films is shown in Fig. 1. The poly(amide amic acid) solutions are made by reacting stoichiometrical amount of p-BAPP, TMAC, BTDA (molar ratio of p-BAPP: TMAC: BTDA = 1: 0.3: 0.7) and suitable amount of DMF under a nitrogen atmosphere and stirring for 2 h. After this period, modified poly(amide amic acid) solutions are prepared by adding the mixture of $Ti(OEt)_4$ and ACAC (molar ratio of Ti $(OEt)_4$ to ACAC is fixed to 1:4) and stirring for 12 h. Pour the poly(amide amic acid) and poly(amide amic acid)/$Ti(OEt)_4$ solutions onto a glass plate, and 250 μm thick film obtained by knife coating and then cured in an air-circulating oven at 60, 100, 150, 200 and 300 °C for each 1 h. Sample abbreviations are named as XT-PAI and XT-PI. X denotes the weight percentage of TiO_2 within polymer matrix and T is represents as the TiO_2. The TiO_2 concentration (X = 2.18, 8.12, 13.20 wt.%) are assuming that complete imidization and complete conversion of the $Ti(OEt)_4$ to the TiO_2. Moreover, the polyimide/titania (PI/TiO_2) hybrid films without TMAC content (molar ratio of p-BAPP: BTDA = 1: 1) are also prepared through the same procedures. The nanocomposite films have an average final thickness of 25–30 μm.

Table 1
Characterization, thermal and mechanical properties of pure PAI, PI, XT-PAI and XT-PI series films

XT-PAI						XT-PI					
X[a]	Quality[b]	DMA test		T_d (°C)[e]	Char yield (%)[f]	X[a]	Quality[b]	DMA test		Td (°C)[e]	Char yield (%)[f]
		(MPa)[c]	T_g (°C)[d]					(MPa)[c]	T_g (°C)[d]		
0	+ +	2023	256.5	555.4	59.3	0	+ +	2010	251.2	523.2	53.6
2.18	+ +	2345	271.3	507.1	63.7	2.18	+ +	2564	276.6	506.1	64.9
8.12	+ +	2683	294.6	496.6	65.1	8.12	− +	3128	310.7	480.5	65.0
13.2	− −	[g]	[g]	466.1	69.0	13.2	[h]	[h]	[h]	[h]	[h]

[a] "X" :TiO_2 wt.%.
[b] "++": flexible; "− +":rigid and tough; "− −"brittle.
[c] Storage modulus of hybrid films are measured at 60 °C.
[d] The maximum in tan δ curve is designated as glass transition temperature.
[e] Temperature at 5 wt.% loss.
[f] Char yield at 800 °C.
[g] The hybrid film is too brittle and fragile to obtain satisfactory measurement.
[h] It can not be synthesized.

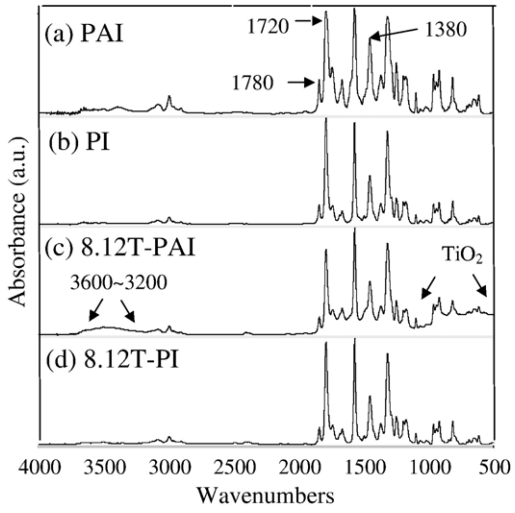

Fig. 2. Fourier transfer infrared spectrophotometer spectra of (a) pure PAI (b) pure PI (c)8.12T-PAI (d) 8.12T-PI nanocomposite films.

2.3. Measurements

Fourier transfer infrared spectrophotometer (FT-IR) absorption spectra are recorded between 4000 and 400 cm^{-1} by Nicolet PROTEGE-460. Scanning electron microscope (SEM) study is carried out with a TESCAN 5136LS focusing on the fractured surfaces of nanocomposite films, which is broken after cooling in liquid nitrogen, and then vapor deposition with a thin gold film. Transmission electron microscope (TEM) data is obtained by JEOL-2000FX. Thermogravimetric analysis (TGA) is performed with a Du Pont TGA-Q500 at a heating rate of 20 °C/min from 60 °C to 800 °C under nitrogen. The dynamic mechanical analysis (DMA) is carried out by means of a thermal analyzer DMA-2980, at a frequency of 1 Hz and heating rate of 3 °C/min. The samples size of 50×5 mm^2. X-ray photoelectron spectrometer (XPS) is obtained by using a VG ESCA scientific theta probe spectrometer working in the constant analyzer energy mode with a pass energy of 28 eV and Al Kα (1486.6 eV) radiation as the excitation source.

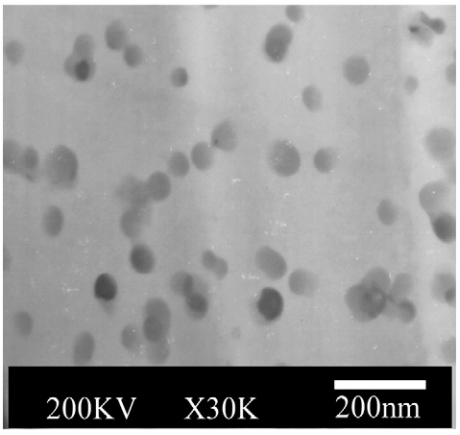

Fig. 3. Transmission electron microscope photograph of the 8.12T-PAI nanocomposite film.

3. Results and discussion

The PAI/TiO_2 and PI/TiO_2 nanocomposite films are obtained by using the sol-gel process. The quality of pure PAI, PI and XT-PAI, XT-PI series films are shown in Table 1. The result indicates that the flexibility and toughness of the TMAC containing 8.12T-PAI nanocomposite film is better than that of 8.12T-PI without TMAC addition. The Fourier transfer infrared spectrophotometer spectra of pure PAI, pure PI, 8.12T-PAI and 8.12T-PI nanocomposite films are shown in Fig. 2. The characteristic peaks of symmetric and asymmetric C═O stretching and C–N stretching of the imide group at 1720, 1780, and 1380 cm^{-1} are observed from all films shown Fig. 2 [1]. TiO_2 has a broad absorption band from approximately 800 to 450 cm^{-1} [11]. While 8.12T-PAI nanocomposite film at 800 to 450 and 3600 to 3200 cm^{-1} have stronger absorption band. It suggests that there is a hydrogen bonding interaction between the NH and the Ti–OH groups, as well as the self hydrogen bonding between the amide C═O and NH in the PAI [9].

The decomposition temperatures (T_d), at 5% weight loss, are listed in Table 1. The result indicates that the decomposition temperature of 5 wt.% loss are all above 460 °C for all hybrid films with TiO_2 content lower than 13.2 wt.% and decreased with the increase of TiO_2 content. According to the previous studies, the decrease in thermal stability could be attributed to

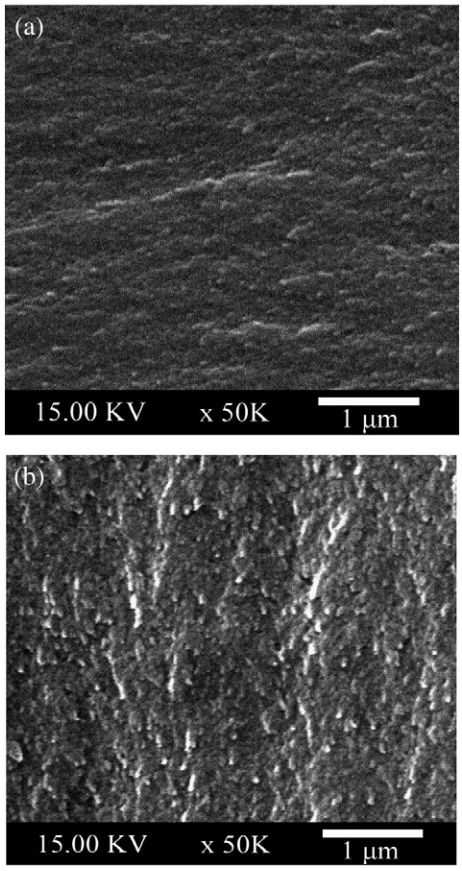

Fig. 4. Scanning electron microscope photographs of the fracture surfaces of (a) 8.12T-PAI (b) 8.12T-PI nanocomposite films.

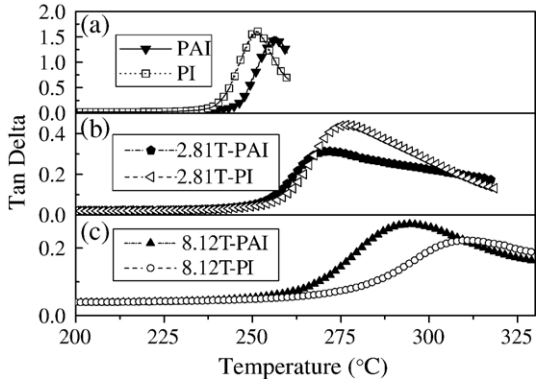

Fig. 5. The tan δ curves of (a) pure PAI and PI (b) 2.81T-PAI and 2.81T-PI (c) 8.12T-PAI and 8.12T-PI nanocomposite films.

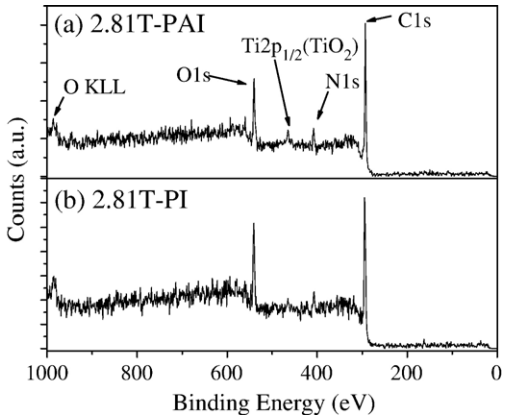

Fig. 6. XPS survey spectra on surface of (a) 2.81T-PAI (b) 2.81T-PI nanocomposite films.

the metallic compounds, which can oxidatively degrade polyimide films (about 460 °C) [12–15]. Although the introduction of TiO_2 causes a decrease in thermal stability, but the char yield after 800 °C decomposition is increased with the increase of TiO_2 content because metal oxide TiO_2 can not decompose in high temperature. All the hybrid films still possess pretty good thermal stability.

The transmission electron microscope micrograph of the fractured 8.12T-PAI nanocomposite film is shown in Fig. 3. Some discrete TiO_2 domains and homogeneously and well-dispersed in PAI matrices are observed obviously. The nano particle sizes of TiO_2 are in the range of 40–90 nm for 8.12T-PAI nanocomposite film. On comparison of Figs. 3 and 4(a), the TiO_2 domain sizes cannot be observed easily in SEM photograph of 8.12T-PAI, whereas they can be detected easily in the TEM photograph, which is more sensitive to the higher-atomic-number Ti. Fig. 4(a) (b) show that 8.12T-PAI possesses more homogeneous cross section than that of 8.12T-PI nanocomposite film and the domain size of these two films are also all small. It is suggested that the incorporation of TMAC also facilitates nano TiO_2 to distribute within PAI matrix.

Table 1 indicates that the storage modulus and glass transition temperature (T_g) of pure PAI is higher than that of pure PI. The main reason may be the intermolecular hydrogen bonding of PAI film. The XT-PAI and XT-PI nanocomposite films with higher TiO_2 content possess superior mechanical property and glass transition temperatures are observed from Table 1 and Fig. 5. The increase of storage modulus is ascribed to the incorporation of TiO_2 forming network structure and increasing the rigidity of the hybrid films [6,8]. From Table 1 and Fig. 5, the glass transition temperature and storage modulus of XT-PI nanocomposite films with the same TiO_2 content are all larger than the corresponding XT-PAI. The reason may be that the hydrogen bonding between PAI and TiO_2 increased, while the hydrogen bonding between PAI and PAI decreased after the addition of TiO_2. By the way, the rotation of amide component, –CONH– single bond structure, will be increased and then the storage modulus and glass transition temperature of XT-PAI films are lower than those of XT-PI films possessed.

The chemical compositions of X-ray photoelectron spectrometer (XPS) of 2.81T-PAI and 2.81T-PI nanocomposite films are shown in Fig. 6. It can be seen that 2.81T-PAI and 2.81T-PI hybrid films contain the compound of Ti $2p_{1/2}$ of TiO_2 (464.9 eV) on the hybrid film surface [16], while the surface of 2.81T-PAI hybrid film for the TiO_2 composite content is more than that of the 2.81T-PI hybrid film. On the other hand, the XPS is a useful technique to monitor polymer–polymer interaction of nitrogen-containing polymers [17–21]. When the nitrogen atom is involved in hydrogen bonding interaction, the binding energy of the N1s electron is increased by about 1.0 eV [21]. Fig. 7 shows the XPS spectra of the N1s binding energy of 2.81T-PAI and 2.81T-PI hybrid films. The N1s spectra of 2.81T-PAI and 2.81T-PI show peak locating at 407.8 eV and 406.7, respectively. This phenomenon is because the addition of TMAC will cause an increase of TiO_2 content on film's surface of 8.12T-PAI. This may be the hydrogen bond structure between amide ground — NH and Ti–OH group of uncompletely condensation between TiO_2. It is implied that the migration of TiO_2 species from the bulk to the surface of the 2.81T-PAI is observed.

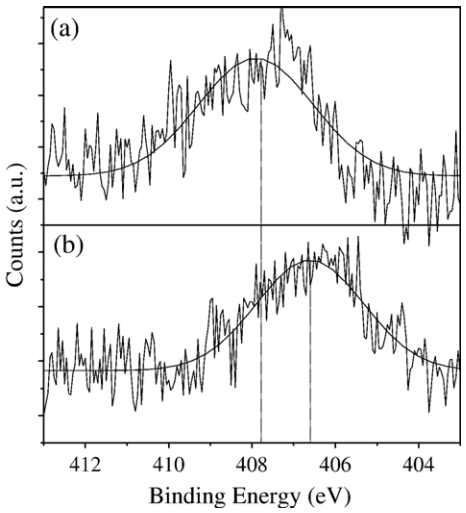

Fig. 7. The N1s component on surface of (a) 2.81T-PAI (b) 2.81T-PI nanocomposite films.

4. Conclusion

Poly(amide–imide)/titania (PAI/TiO_2) and polyimide/titania (PI/TiO_2) nanocomposite films are synthesized by sol-gel technology. The TMAC is added to the synthesis of poly (amide–imide)/TiO_2 films for the formation of intermolecular hydrogen bonding that will influence the surface characteristics, morphology and mechanical properties. The result indicates that as the TMAC containing, the flexibility and toughness of the 8.12T-PAI nanocomposite film is formed and the TiO_2 is well-dispersed within PAI matrix. Due to the XPS analysis, the TiO_2 content on the surface of 2.81T-PAI is higher than that of 2.81-PI nanocomposite film. The PAI/TiO_2 and PI/TiO_2 nanocomposite films with higher titania content exhibits higher glass transition temperature and storage modulus than pure PAI and PI. Although the thermal stability of the nanocomposite films are decreased by introducing TiO_2, but the nanocomposite films still reveal pretty good thermal resistance.

Acknowledgements

The authors would like to express their appreciation to the National Science Council of the Republic of China and Taimide Technology Company for financial support for this study under grant NSC- 95-2622-E-167-007-CC3.

References

[1] J.E. Mark, C.Y.C. Lee, P.A. Bianconic (Eds.), ACS Symposium Series 585, hybrid organic–inorganic composites, American Chemical Society, Washington DC, 1995.
[2] M.K. Ghosh, K.L. Mittal (Eds.), Polyimide Fundamentals and Applications, chapter 3, New York, 1996.
[3] J.R. Devore, J. Opt. Soc. Am. 41 (1951) 416.
[4] J.M. Bennett, E. Pelletier, G. Albrand, J.P. Borgogno, B. Lazarides, C.K. Carniglia, R.A. Schmell, T.H. Allen, T. Tuttle-Hart, K.H. Guenther, A. Saxer, Appl. Opt. 28 (1989) 3303.
[5] W. Que, Y. Zhou, Y.L. Lam, Y.C. Chan, C.H. Kam, Thin Solid Films 358 (2000) 16.
[6] P.C. Chiang, W.T. Whang, M.H. Tsai, Thin Soild Films 447 (2004) 359.
[7] P.C. Chiang, W.T. Whang, S.C. Wu, K.R. Chuang, Polymer 45 (2004) 4465.
[8] M.H. Tsai, S.J. Liu, P.C. Chiang, Thin Solid Films 515 (2006) 1126.
[9] Q. Hu, E. Marand, Polymer 40 (1999) 4833.
[10] K. Ebert, D. Fritsch, J. Koll, C. Tjahjawiguna, J. Membr. Sci. 233 (2004) 71.
[11] R.A. Nyquist, R.O. Kagel, Infrared Spectra of Inorganic Compounds, Academic Press, New York, 1971 (214).
[12] T. Sawada, S. Ando, Chem. Mater. 10 (1998) 3368.
[13] R.K Boggess, L.T. Taylor, J. Polym. Sci., Polym. Chem. Ed. 25 (1987) 685.
[14] J.D. Rancourt, L.T. Taylor, Macromolecules 20 (1987) 790.
[15] M.H. Tsai, C.J. Ko, Surf. Coat. Technol. 201 (2006) 4367.
[16] C. Boulmer-Leborgne, J. Hermann, B. Dubreuil, P. Brault, M.L. DeGiorgi, G. Leggieri, A. Luches, M. Martino, A. Perrone, I.N. Mihailescu, I. Ursu, Blondiaux, J.L. Debrun, H. Estrade, B. Rousseau, Appl. Surf. Sci. 54 (1992) 349.
[17] X. Zhou, S.H. Goh, S.Y. Lee, K.L. Tan, Appl. Surf. Sci. 119 (1997) 60.
[18] X. Zhou, S.H. Goh, S.Y. Lee, K.L .Tan, Appl. Surf. Sci. 126 (1998) 141.
[19] X. Zhou, S.H. Goh, S.Y. Lee, K.L .Tan, Polymer 39 (1998) 3631.
[20] C.M. Chan, L.T. Weng, Rev. Chem. Eng. 16 (2000) 3641.
[21] M. Wang, K.P. Pramoda, S.H. Goh, Carbon 44 (2006) 613.